

# THE 4TH INTERNATIONAL CONFERENCE ON ALUMINUM ALLOYS

## **DEFORMATION MICROSTRUCTURES AND PSN IN HOT-WORKED ALUMINIUM ALLOYS**

S. Sircar and F.J. Humphreys  
Manchester Materials Science Centre,  
Grosvenor Street, Manchester M1 7HS, England.

### Abstract

Annealed samples of a number of aluminium alloys including 3003 and 1050 were deformed in uniaxial compression over a wide range of strain, strain rate and temperature and subsequently recrystallised. The conditions for the formation of deformation zones adjacent to large particles are found to be in agreement with the Humphreys-Kalu theory for all the alloys with the exception of the solutionised 3003 alloy. This is believed to be due to slow climb of dislocations due to strong dislocation-solute interactions. The conditions for particle stimulated nucleation of recrystallisation following hot deformation was also investigated. Particles at the grain boundaries were found to be more efficient sites for particle stimulated nucleation. There is some evidence of the association of particles with nuclei under deformation conditions where deformation zones were not observed. The possible reasons for this behaviour have been outlined.

### Introduction

The hot deformation and subsequent annealing behaviour of non heat-treatable aluminium alloys is of great commercial interest. The behaviour of a series of particle-containing aluminium alloys deformed by different methods and under different conditions is being studied in a European Community funded project (BREU- CT 91-0399 (MNLA)), and as part of this project, the current paper describes some preliminary results of experiments aimed at obtaining fundamental information on the deformation and annealing behaviour of these materials at low rates of strain.

### Materials and methods

The materials used in this research were Al-1Mn, Al-1Mg and commercial purity aluminium (AA1050) alloys. The compositions of the alloys are as shown in table I. The

large eutectic particles of about  $5.5\mu\text{m}$  size were mainly FeSi and  $\text{Fe}_3\text{Al}$ . In the Al-Mn alloy, there were also small dispersoids of  $\text{MnAl}_6$  which were approximately  $1\mu\text{m}$  in size. Some details of the volume fractions, mean sizes and size range of the large particles are given in table I.

**Table I. Materials Data**

Material	Composition (wt%)				Volume fraction(%)	Av. size + largest size( $\mu\text{m}$ )
	Fe	Si	Mn	Mg		
Al-Mn	0.37	0.15	1.01		3.84	5.43+18
Al-Mg	0.33	0.15		0.98	0.91	4.05+28
1050	0.32	0.15			0.82	3.53+14

The materials were solutionised at  $600^\circ\text{C}$  for 40 mins and water quenched. The Mn in solid solution was 0.6 weight percent as determined by resistivity measurements. For comparison, samples of the Al-Mn alloy were also furnace cooled from  $600^\circ\text{C}$  to  $200^\circ\text{C}$  at  $10^\circ\text{C/hr}$  in order to precipitate most of the Mn.

Rectangular compression specimens of  $10\times 10\times 20$  mm were deformed by uniaxial compression in an Instron testing machine at strain rates between  $10^{-5}/\text{s}$  and  $10^{-1}/\text{s}$  and at temperatures between room temperature and  $500^\circ\text{C}$ . The specimens described in the present paper were all deformed to a true strain of 0.7. The specimens were rapidly quenched at the end of the test in order to retain the deformed microstructure.

The deformed specimens were sectioned parallel to the compression direction and were mechanically polished, electropolished and anodised to reveal the grain structure under polarised light. Further microstructural analysis was carried out by scanning and transmission electron microscopy and diffraction.

## Results and discussion

### The deformation microstructure

After deformation at elevated temperature and low strain rates (low Zener-Hollomon parameter Z), the microstructures consisted of regular arrays of large, well-defined subgrains and the particles appear to have very little effect on the deformed microstructure (figure 1).

However, at lower temperatures and higher strain rates (high Z), the microstructure is very irregular consisting of fine scale deformation bands and local lattice rotations around

large particles. Figs. 2-5 show the typical intermediate temperature deformation microstructure in the different materials. The Al-Mg alloy shows fine scale deformation bands (figure 2) and the 1050 alloy shows a more regular substructure (figure 3). The precipitated Al-Mn alloy show a irregular structure with substructure associated with particles (figure 4). Figure 5 shows typical lattice rotations around particles in the solutionised Al-Mn alloy.

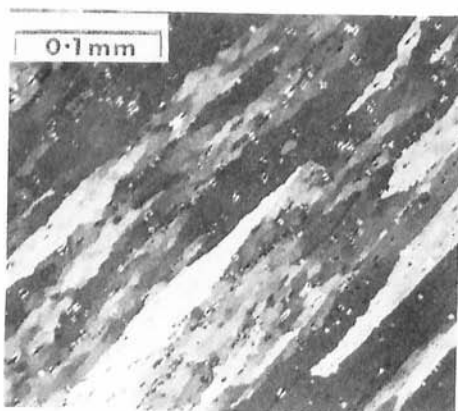


Fig. 1. Optical micrograph of Al-Mn(soln) deformed at 400°C,  $10^{-4}$ /s showing well defined subgrains.

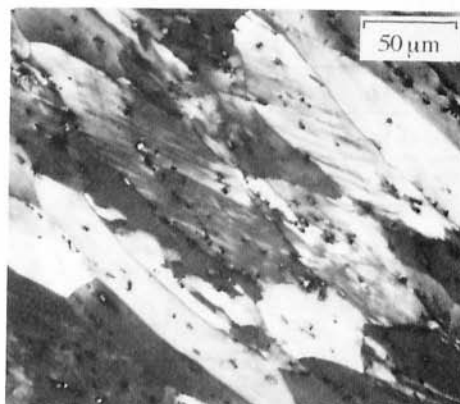


Fig. 2. Optical micrograph of Al-Mg(soln) deformed at 200°C,  $10^{-3}$ /s showing deformation bands.

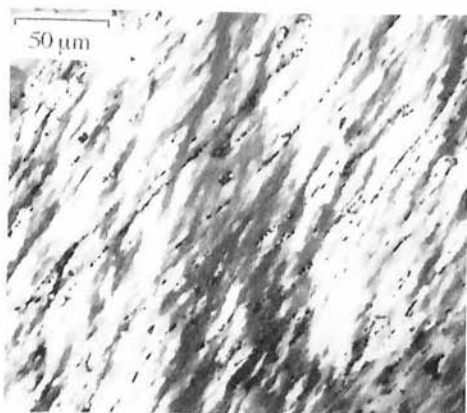


Fig. 3. Optical micrograph of 1050 alloy deformed at 250°C,  $10^{-3}$ /s showing a regular substructure.

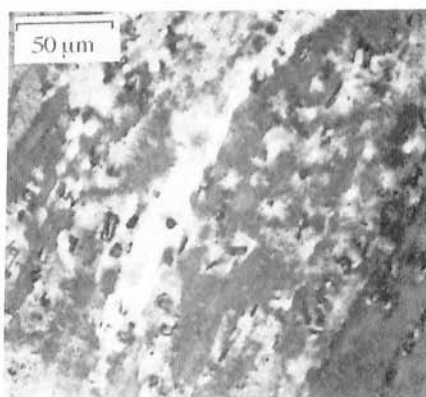


Fig. 4. Optical micrograph of Al-Mn(ppt) deformed at 300°C,  $10^{-2}$ /s showing deformation zones around particles.

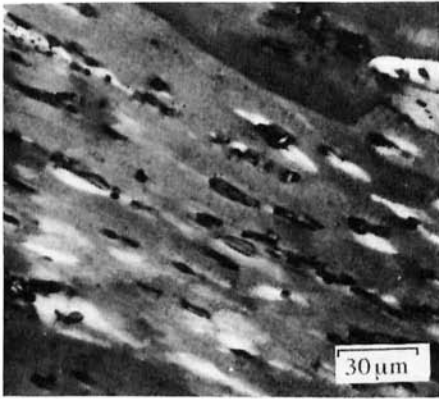


Fig. 5. Optical micrograph of Al-Mn(sol) deformed at 300°C, 10<sup>-3</sup>/s showing lattice rotations around particles.

The conditions under which local lattice rotations were observed adjacent to the large particles were determined as a function of deformation temperature and strain rate. The transition temperature above which deformation zones were not observed is shown as a function of strain rate in figure 6.

Humphreys and Kalu (1) found that the transition in Al-Si alloys for particles of diameter  $d$  was given by

$$\dot{\epsilon}_c = \frac{K_1 \exp(-Q_v/RT)}{Td^2} + \frac{K_2 \exp(-Q_b/RT)}{Td^3} \dots \dots \dots (1)$$

where  $K_1$  and  $K_2$  are derived constants,  $Q_v$  and  $Q_b$  are the activation energies for bulk and surface diffusion,  $d$  is the particle size,  $R$  is the gas constant and  $T$  is the temperature.

It is significant that the data for all the alloys with the exception of the quenched Al-Mn samples lie very close to the line defined by equation 1 for a particle diameter of 5 μm. The transition temperature for the quenched Al-Mn samples is some 50°C higher, indicating according to the analysis on which equation 1 is based, that climb of dislocations around the particles is much slower in this material. Microstructural investigations have shown that this is not due to the inhibiting effects of fine-scale precipitation during deformation and we therefore conclude that the retardation of climb is due to manganese in solid solution. It is interesting to note from figure 6 that although 1% of manganese in solid solution has a marked effect, 1% of magnesium, which is an element known to strongly pin dislocations, appears to have little effect although it has been reported that in Al-5%Mg, there is some increase in the transition temperature (2). The reasons for the increase in the transition temperature caused by solutes are not entirely clear, but are tentatively ascribed to solute-vacancy binding effects (3,4).

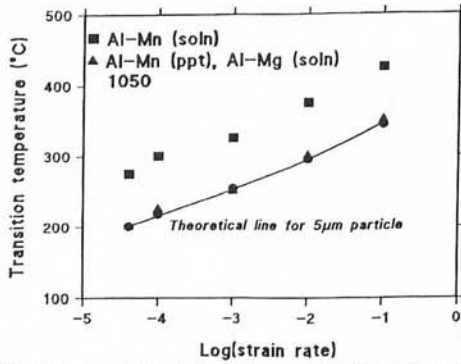


Fig. 6. Microstructural transition as a function of strain rate.

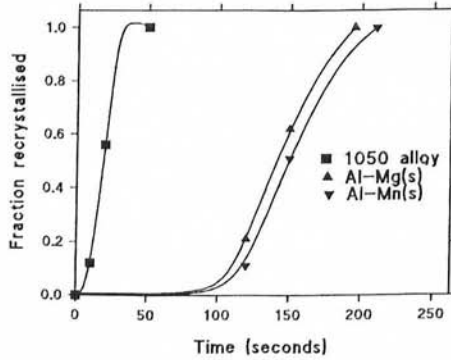


Fig. 7. Comparison of recrystallisation kinetics of different materials.

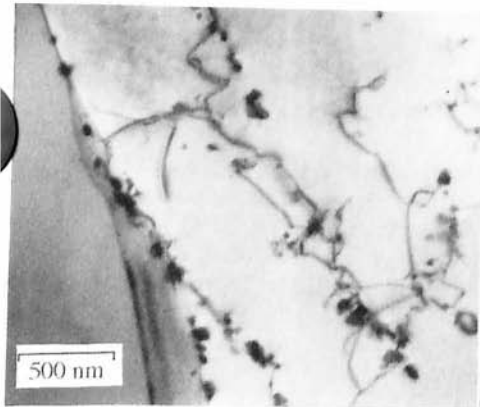


Fig. 8. TEM micrograph of Al-Mn(soln) alloy deformed at 200°C and annealed at 400°C showing precipitation of fine particles.

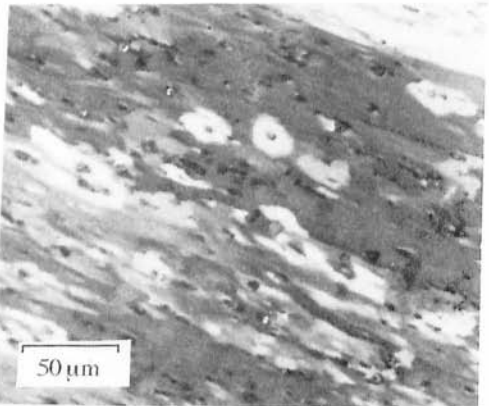


Fig. 9. Optical micrograph of Al-Mn(soln) alloy deformed at 25°C and annealed at 375°C showing PSN.

There was no evidence of any particle-stimulated dynamic recrystallization in any of the alloys under any of the deformation conditions. This is consistent with the results of Kalu and Humphreys (5), and differs from those of Castro-Fernandes and Sellars (6) who reported some evidence of this phenomenon in Al-1Mn-1Mg.

### Annealing behaviour

The deformed specimens were subsequently annealed in a salt bath. The recrystallization kinetics for specimens deformed at 200°C and then annealed at 400°C is shown in figure 7. The much slower recrystallization of the solutionised Al-Mn and Al-Mg alloys compared to the 1050 alloy is thought to be due to precipitation at dislocations and boundaries which occurred during the annealing of these materials as shown in figure 8.

Particle-stimulated nucleation of recrystallization (PSN) as shown in fig. 9 at a high Z (Zener-Hollomon parameter) is an important mechanism of interest, and the occurrence of PSN was investigated as a function of deformation conditions and deformation microstructure.

The number of nuclei - Table II shows that the fraction of particles clearly associated with nuclei (the PSN efficiency) in the early stages of recrystallization is quite small, typically less than 0.15. The final grain size of the alloys after recrystallisation at high Z is of the order of 45µm which again indicates a PSN efficiency of 0.3. This differs from results for alloys containing small numbers of large particles (7,8) where the PSN efficiency is close to 1, but is in agreement with other work on alloys containing larger numbers of particles (9) where a low efficiency of PSN is commonly found. The reason for the low PSN efficiency is likely to be due to either the absence of a suitable deformation structure for PSN at some particles or to the number of nuclei increasing with time as opposed to there being site-saturated nucleation which is often assumed to occur for PSN (10).

The effect of the particle site - A comparison of the nucleation efficiency at particles situated either within a grain or at a grain boundary is given in table II, where it may be seen that particles at a grain boundary are more likely to nucleate recrystallization than those within the grain by a factor of ~2 (Al-Mn) to ~4 (1050). This is in agreement with the observation of Bay and Hansen on cold worked and annealed commercial purity aluminium (11). There are two factors which may contribute to this. Firstly, the local strains near grain boundaries often differ from those in the grain interiors and secondly, the pre-existing high angle grain boundary is likely to make the development of a nucleus easier and more rapid.

**Table II. Particle stimulated nucleation at grain boundaries in specimens deformed at high Z and recrystallized ~10%.**

Material	Total number of particles counted	Particles at grain boundaries(%)	Total number of nuclei counted	Nucleation at grain boundary particles(%)
Al-Mn (sat)	2043	7.5	387	16
Al-Mn (ppt)	2003	16	295	30
Al-Mg	1047	20	303	55
1050	1931	17	281	75

The effect of the deformation conditions - Although as seen from figure 6 deformation zones were not observed above a critical temperature, there was some evidence of the association of recrystallization nuclei and particles at higher temperatures as shown in figure 10.

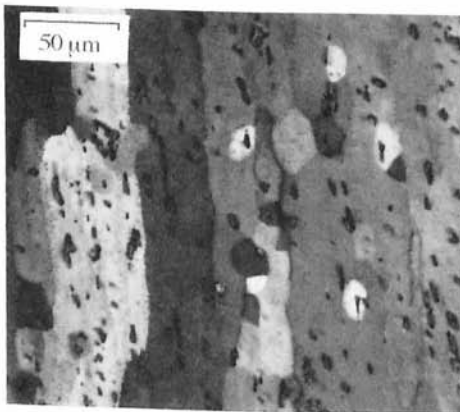


Fig. 10. Optical micrograph of Al-Mn (soln) alloy deformed at 400°C, 10<sup>-3</sup>/s annealed at 525°C showing association of particles with nuclei.

This behaviour was not found by Oscarrson et. al (12) nor Kalu and Humphreys (13). Possible reasons for this include:

*-The association between particles and nuclei is one of chance.* With a large number of particles the chances of observing a nucleus in contact with a particle are large. A simple statistical analysis given in appendix A shows that a growing grain of diameter 20µm in the Al-Mn alloy containing a volume fraction of 0.03 of 5.5µm diameter particles has a probability of 0.43 of touching a grain.

*-Larger particles retain a deformation zone to higher deformation temperatures.* In addition to the mean particle diameter, table 1 also shows the maximum particle size observed in all the alloys. Equation 1 shows that for a strain rate of 10<sup>-3</sup>/s particles of

diameter  $20\mu\text{m}$  would retain a deformation zone to a temperature approximately  $50^\circ$  higher than for  $5\mu\text{m}$ .

### References

1. F.J. Humphreys and P.N. Kalu, Acta Met., Vol. 35, No.12, p2815, 1987.
2. P.N. Kalu and F.J. Humphreys, Aluminium Tech.'86, March 1986, London, p197.
3. V.C. Kannan and G. Thomas, Jour. of Appl. Physics, 37, No.6, p2363, 1966.
4. G. Hausch, P. Furrer and H. Warlimont, Z. Metallkde., p69, 1978.
5. P.N. Kalu and F.J. Humphreys, Proc. 7th Int. Riso Symp., Roskilde, p385, 1986.
6. F.R. Castro-Fernandez and C.M. Sellars, Mat. Sci. and Tech., No.4, p621, 1988.
7. F.J. Humphreys, Acta Met., 25, p1323, 1977.
8. F.J. Humphreys, Recrystallization'90, Ed. T. Chandra, The Minerals, Metals and Materials Society, p113, 1990.
9. J.A. Wert, N.E. Paton, C.H. Hamilton and M.W. Mahoney, Met. Trans A, 12A, p1267, 1981.
10. E. Nes, 1st Int. Riso Symp., Denmark, p85, 1980.
11. B. Bay and N. Hansen, Met. Trans A, Vol 10A, No.3, p279, 1979.
12. A. Oscarrson, W.B. Hutchinson and A. Karlsson, 8th ILMT, (Leoban, Vienna), p531, 1987.
13. P.N. Kalu and F.J. Humphreys, 10th Int. Riso Symp., Denmark, p415, 1989.

### Appendix A

Take a cube of length  $G$  (final grain diameter).

Volume of cube =  $G^3 = V_c$

$X \cdot V_c = V_r$  (where  $X$  is the fraction recrystallised and  $V_r$  is the volume of partially recrystallised grains)

Radius of partially recrystallised grains =  $R = (X \cdot V_c \cdot 3/4\pi)^{1/3}$

No. of particles per unit volume =  $3F_v/4\pi P^3 = N_v$  (where  $P$  is the particle size and  $F_v$  is the volume fraction of particles)

No. of particles in the cube =  $N = N_v \cdot V_c$

Particle touches recrystallised grain if it is within  $R$ .

Therefore the particle touches if it is within a volume  $E = 4\pi (R)^3/3$

Taking the effect of sectioning into account, the chances of a particle being associated with a nuclei is  $N \cdot E \cdot P / V_c \cdot R = F_v \cdot R^2 / P^2$